Conference paper

Stefan Hoffmann, Juan Pablo Fuenzalida Werner, Ignacio Moreno-Villoslada* and Francisco M. Goycoolea*

New insights into the nature of the Cibacron brilliant red 3B-A – Chitosan interaction

DOI 10.1515/pac-2016-0712

Abstract: Cibacron brilliant red 3B-A (CBR) has been introduced to determine chitosan (CS) concentrations in solution, and several studies applied it to measure chitosan content in pharmaceutical formulations. So far, studies have relied on the absorbance band shift to 570 nm to determine the extent of the CBR – CS interaction. In this study, we show that CBR forms micro- to nanometer sized aggregates with CS, depending on their charge ratio and that other photophysical changes in CBR are induced by this interaction. We found that, besides the bathochromic band shift, aggregation induces emission at 600 nm and emission quenching at 360 nm. We compared changes CS induced in absorbance and fluorescence emission of CBR with the CS monomer glucosamine and poly(allylamine) hydrochloride, which both contain amino groups, and found that similar but less intense photophysical changes also occur. Furthermore, CS-induced circular dichroism in CBR suggests a twisted, chiral structure of these aggregates that should match with the previously published *in silico* simulations of the structure of CS in solution. The low linear charge density of CS and its chiral conformation are considered responsible for the enhanced photophysical response of CBR interacting with the polycation.

Keywords: aggregation; chitosan; dye interaction; EUCHIS-12; ICCC-13; polyelectrolyte–dye interactions; polyelectrolytes.

Introduction

Chitosan (CS) is chemically produced at large scale by thermoalkaline deacetylation of chitin, a widely abundant natural polymer found on earth that is produced by numerous organisms like fungi, arthropods, crustaceans, insects and mollusks. The deacetylation reaction frees the amino groups in the polymer which can be protonated in acidic conditions, making CS the only positively charged naturally sourced polymer [1]. This polycationic character is important in many of the numerous applications it finds in multiple fields. Examples include the interaction with negatively charged nucleic acids to form polyplexes for gene delivery or in facilitating the interaction with negatively charged mucosa and cell membranes for drug delivery vehicles and the interaction with crosslinking agents to form hydrogels, to name a few [2–4].

Metachromasy (also referred to as metachromasia) is a phenomenon discovered in the middle of the 19th century where a chromotrope induces a change in the absorbance spectrum of a chromophore. Both

Article note: A collection of invited papers based on presentations at the 12th Conference of the European Chitin Society (12th EUCHIS)/13th International Conference on Chitin and Chitosan (13th ICCC), Münster, Germany, 30 August – 2 September 2015.

***Corresponding authors: Ignacio Moreno-Villoslada,** Instituto de Ciencias Químicas, Facultad de Ciencias, Universidad Austral de Chile, Casilla 567, Valdivia, Chile, e-mail: imorenovilloslada@uach.cl; and **Francisco M. Goycoolea,** IBBP, Westfälische Wilhelms-Universität Münster, Schloßgarten 3, 48149 Münster, Germany, e-mail: goycoole@uni-muenster.de
Stefan Hoffmann and Juan Pablo Fuenzalida Werner: IBBP, Westfälische Wilhelms-Universität Münster, Schloßgarten 3, 48149 Münster, Germany

hypsochromic and bathochromic shifts of absorbance bands have been observed. Initially, it was mainly used in microscopy for specifically staining tissues; later it was found that many dyes interact with polyelectrolytes (PELs) of opposite charge in solution and the same effect was observed [5]. Although it was first thought that the chromotropes are always anionic and the dyes cationic, shortly after, examples of the reverse case were found [5, 6]. PEL – dye interactions are mostly governed by the electrostatic interaction of either cationic or anionic dyes with oppositely charged PELs. The second type of interaction are hydrophobic in nature and can be found either between hydrophobic sites in the PELs with a dye molecule or between the dye molecules. In some cases, aromatic-aromatic (π–π) interactions can also be an important factor as studied in methylene blue – sulfonated PELs and rhodamine 6G – polyanions [7–9]. Spectral changes of the dyes are often thought to be due to the π–π interactions of the dye with other dye molecules or the PEL. Solvatochromic effects in water due to preferential solvation are also considered, both with organic solvents residues and with amphiphilic polymers [10]. Some dyes not showing metachromatic effects during interaction with oppositely charged PELs could be interacting through long-range electrostatic interactions, without releasing water from their hydration sphere, therefore not showing spectral changes [11].

The relative orientation of aggregated dye molecules has been used to explain their photophysical behavior. According to the exciton theory upon dye dimerization, the excited state of the monomer is split into two excited energy states (S_1 and S_2) of which only one is allowed depending on the type of aggregate. The slip angle (θ) is the relative orientation of the dyes in a dimer. In a parallel, sandwich-like dimer with a large slip angle, a higher excited state than in the monomer has to be reached. Since the energy required is higher, shorter wavelength light is required to reach the excited state, and the absorbance spectra will show a hypsochromic shift. These types of dimers have been named H-aggregates (H for hypsochromic) and the corresponding absorbance bands H-bands. A head-to-tail or staggered dimer has a lower slip angle and the excited state that can be reached has a lower energy than the excited monomeric state. This means that the absorbance spectra will show a bathochromic shift to a higher wavelength. These dye-dimers have been named J-aggregates (J for Jelley, one of the first describers) and the corresponding absorbance bands J-band [12–17]. Taking into account the angle between the transition moments of both monomers in a dimer (α), both H- and J-bands will be observed in the absorption spectra for a twisted sandwich-like or oblique head-to-tail dimer [18].

Cibacron brilliant red 3B-A (Reactive Red 4, C.I. 18105, from here on CBR) is a high molecular weight monoclorotriazin dye that was selected for a colorimetric method to determine CS concentration in solution. It possesses four sulfonate groups that make the otherwise mainly hydrophobic molecule soluble in aqueous media and give it four negative charges per molecule. CBR was used for inactivation of yeast kinase phosphotransferase activity. It was concluded that the dye inhibits the enzyme by active site inactivation and that hydrophobic interactions are the driving factor [19]. CBR was later selected from a number of dyes as suitable for a colorimetric method to determine CS concentrations in solution. In contrast to Cibacron Blue F3GA, CBR did not show deviation from the Beer's law at the concentrations explored [20, 21]. It was shown that the interaction between CBR and CS induced a linear absorbance increase at 570 nm with increasing CS concentration, a fact that has been proposed as a method to determine CS concentration in solution, to which we will refer to as the colorimetric method. This method was also used for the first quantitative analysis of pharmaceutical CS formulations and was found to be simple, cost-effective and fast [22]. However, separate calibration curves for different CSs have to be created, probably because of the diversity in degree of acetylation (DA) and accessibility of the polymer depending on the molecular weight (MW) [21]. An improvement of the original colorimetric method has been proposed by changing the procedure so as not to measure the intensity of the new absorbance band. After centrifuging the colloids created by the interaction between CS and CBR, the concentration of CBR was determined by measuring the original absorbance band of the dye that was not interacting with CS, a method to which we will refer to as the centrifugation method. The sensitivity was increased up to 2 ppm [23].

While previous studies have addressed the application of the CBR – CS interaction, in the present one, we pursuit to glean a deeper understanding of the mechanism of the interaction. Therefore, we used dynamic light scattering to study colloidal aggregation of CBR – CS complexes regarding size and zeta potential. Aggregate

size and zeta potential are important factors in determining the colloidal stability that will influence how complexes sediment during centrifugation, which was used in the revised method to study unbound dye [23]. Additionally, circular dichroism and fluorescence spectroscopy will be used to explore further how the aggregation affects the photophysical behavior of the dye. Glucosamine, the monomer that makes up chitosan and poly(allylamine) hydrochloride (PAH), a synthetic cationic polymer containing primary amines, will be used to check the specificity of the photophysical effects induced by the interaction of CBR with CS.

Materials and methods

Materials

Chitosan HMC 70/5 with a degree of acetylation of 32 % and viscosimetric molecular weight of 17.6 kDa was obtained from Heppe Medical Chitosan GmbH (Halle, Germany). Poly(allylamine) hydrochloride (PAH) with a molecular weight of 900 kDa as specified by the supplier and D(+) glucosamine hydrochloride with a specified purity of ≥ 99 % were obtained from Sigma Aldrich (SA, St. Louis, USA). Cibacron brilliant red 3B-A was purchased from Santa Cruz Biotechnology without specified purity (SCB, Dallas, USA). An older dye stock of CBR, purchased from Sigma Aldrich (SA, St. Louis, USA), which is not available for purchase anymore specified a dye content of 50 %. We compared both dye stocks in absorbance measurements at the same concentration and found almost no difference. Experiments in this work were performed with SCB CBR since it is still available for purchase and we assume a dye content of 50 % for concentration and molar charge calculations. All other reagents were of highest purity if not stated otherwise. The structure of the molecules used in this study is shown in Fig. 1.

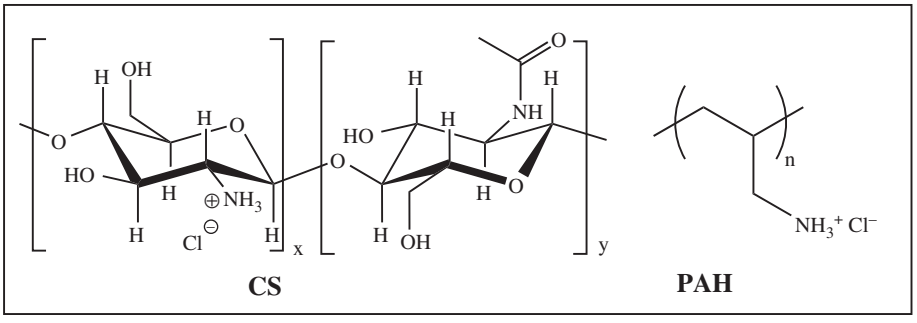

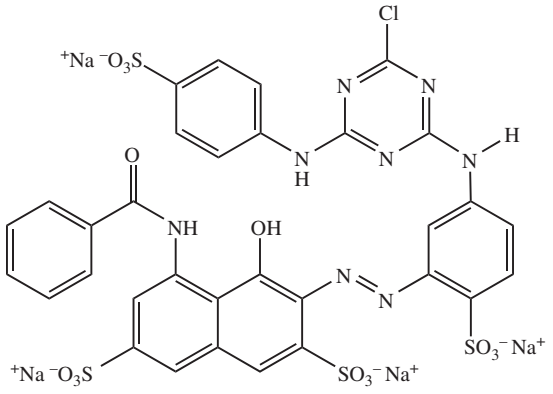

Fig. 1: Molecular structures of the PELs used and CBR.

Methods

All measurements were performed with glycine-HCl buffer 0.1 M as described by Muzzarelli [21]. CBR concentration was fixed at a concentration of 0.075 g/L while CS concentrations were varied.

Dynamic light scattering analysis. Particle size and polydispersion index were determined by dynamic light scattering with non-invasive back scattering (DLS-NIBS) at a measurement angle of 173 °. The zeta potential was measured by mixed laser Doppler velocimetry and phase analysis light scattering (M3-PALS). A Malvern Zetasizer NanoZS (Malvern Instruments, Malvern, UK) fitted with a red laser ($\lambda = 632.8$ nm) was used for both types of measurement.

Absorbance spectroscopy. Absorbance spectra were recorded using a JASCO V-630 Spectrophotometer (Groß-Umstadt, Germany) with 1 mL Hellma quartz cells (Mühlheim, Germany) with a light path length of 10 mm. Spectra of CBR in interaction with CS were recorded using glycine-HCl buffer as baseline and with a CBR concentration of 0.075 g/L. Comparisons of CBR in interaction with CS, glucosamine and PAH were performed using a Tecan Safire Microplate reader (Crailsheim, Germany) using Greiner Bio-One UV-star black microplates (Kremsmünster, Austria). Absorbance spectra deconvolution was performed using Fityk with wavelength converted to energy [24].

Fluorescence spectroscopy. Fluorescence 3D scans were performed in a Jasco FP-6500 (Groß-Umstadt, Germany). Comparisons of CBR in interaction with CS, glucosamine and PAH were performed using a Tecan Safire Microplate reader (Crailsheim, Germany) using Greiner Bio-One UV-star black microplates (Kremsmünster, Austria) in top reading mode. All fluorescence intensities were divided by the sample absorbance at the excitation wavelength to obtain responses proportional to the quantum yield. Fitting of fluorescence data was performed using one-phase linear decay fit and binding saturation one site fit which are built into GraphPad Prism (San Diego, USA).

Circular dichroism spectroscopy. Conformational changes of CBR were analyzed using an AVIV 400 Circular Dichroism Spectrophotometer (Lakewood, USA). The samples were placed in 1-mm quartz cuvettes, and the spectra were recorded at 25 °C and a scanning speed of 200 nm/min from 650 nm to 200 nm, with a response time of 1 s and a bandwidth and data pitch of 1 nm. All spectra were subtracted by a spectrum of the glycine-HCl buffer which served as baseline. Second order smoothing of spectra was performed using GraphPad Prism (San Diego, USA) with 10 neighbors.

Results and discussion

CBR and CS form micro- to nanocomplexes upon interaction

Previous studies of the CBR – CS interaction focused on the spectroscopic analysis, mostly to determine CS concentration in solution using the colorimetric method [21–23, 25]. In this work, we aim to glean a deeper understanding of the interaction by previously unused techniques. Mendelovits et al. observed negative, neutral and positively charged colloidal particles depending on dye – polymer ratios [23]. Based on these findings we performed dynamic light scattering analysis of CBR – CS complexes to investigate their colloidal properties. The particle size, count rate and zeta potential analysed at different dye – polymer ratios are shown in Fig. 2.

The measured values of zeta potential analysis were consistent with previously reported particle charges. We found that at NH_3^+/SO_3^- ratios lower than one, aggregates showed a negative zeta potential of –12 mV shifting to neutral at a ratio of about one. At higher ratios, the zeta potential was found to be +20 mV with no further change regardless of NH_3^+/SO_3^- ratio.

The particle size analysis has shown micrometer-sized aggregates at low NH_3^+/SO_3^- ratios with the largest sizes measured around neutral zeta potential. At higher ratios, the aggregates decreased in size to about 100 nm. Similar to the result in size, the count rate had its peak in the neutrality point and was found lower

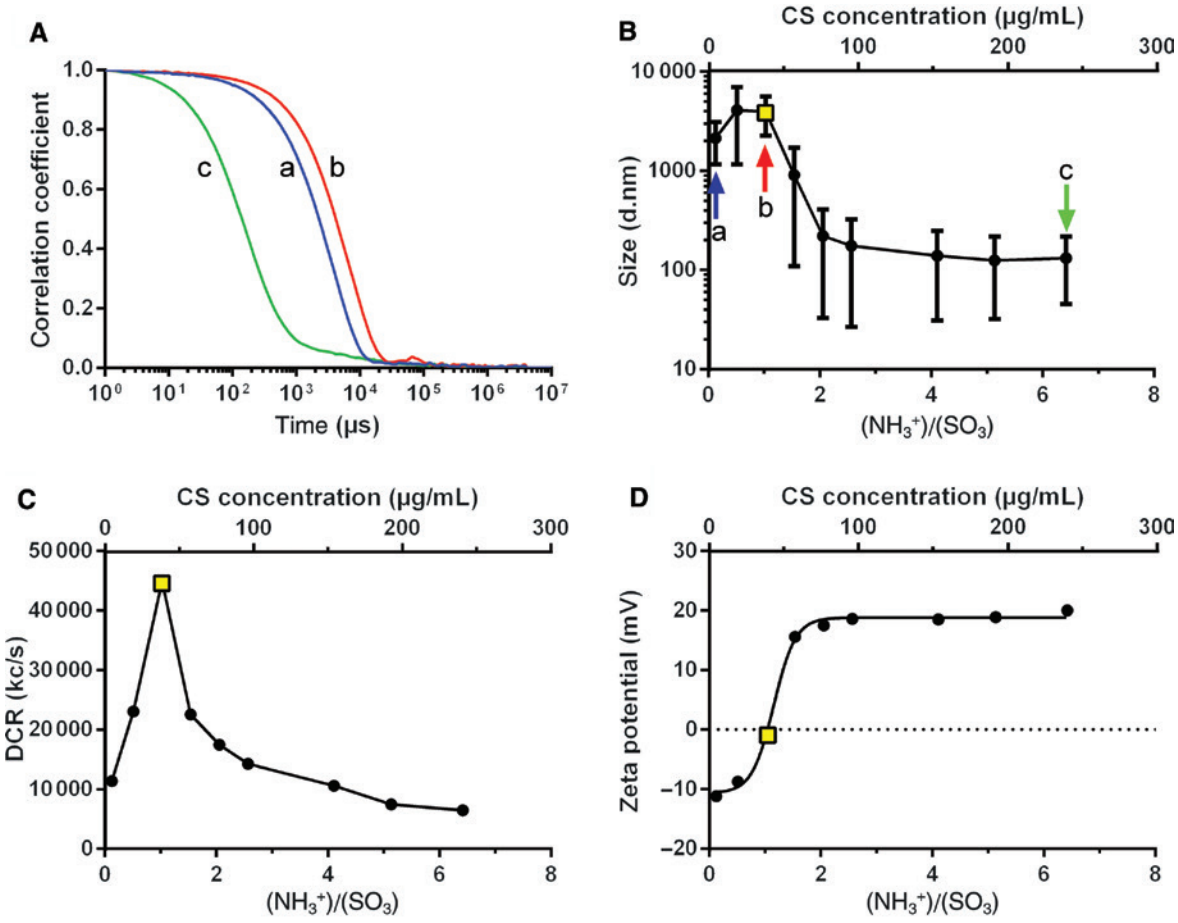

Fig. 2: (A) Exemplary DLS-NIBS correlograms of three size measurements indicated by arrows in B, (B) Size of CBR – CS complexes with standard deviation showing polydispersity in nanometers (PDI width), (C) Derived count rate, (D) Zeta potential versus CS NH_3^+ to CBR SO_3^- ratio. The measurement at the NH_3^+/SO_3^- ratio approaching a zeta potential of 0 mV is indicated by the square symbol in graphs B–D. All measurements performed with 0.075 g/L CBR in glycine-HCl buffer (pH 3.22, 0.1 M) with varying concentrations of CS, expressed in NH_3^+/SO_3^- charge ratio and CS concentration in µg/mL.

at higher and lower NH_3^+/SO_3^- ratios. These features reveal the highly electrostatic nature of the interaction between both molecules. Also, it is remarkable that the micro- and nanocomplexes formed can involve an excess of the dye, thus furnishing a net negative zeta potential to the assemblies.

The revised method [23] to determine CS concentration in solution (the centrifugation method) proposed the use of centrifugation to separate CBR-CS colloids from unbound dye. Afterwards, the concentration of unbound dye was determined to linearly correlate with CS concentration and showed an improved sensitivity compared to the colorimetric method. Our size and zeta potential measurements confirmed differences on the colloidal stability of the CBR – CS complexes. Although sedimentation of CBR – CS aggregates in samples with low or neutral zeta potential easily occurs, increased colloidal stability, owing to the positive zeta potential and lower size (around 150 nm) of the complexes at high NH_3^+/SO_3^- ratios, may produce a residual amount of complexed dye in solution after centrifugation. Thus, the revised centrifugation method showed a linear decrease in dye up to 20 µg/mL of CS, but after centrifugation at concentrations higher than 20 µg/mL the authors found an increase in the amount of dye in solution [23]. This is explained by the higher stability of the colloids furnished by the increasing concentration of the polycation, as shown in this work, a fact that must be taken into account when using the centrifugation method to determine CS concentrations outside the linear range.

Photophysical changes induced in CBR upon interaction with CS

As previously reported, CBR absorbance shows a bathochromic shift from a plateau from 520 nm to 550 nm to two distinct peaks at around 530 nm and 570 nm. The latter shows a linear increase with CS concentration from 5 µg/mL to 50 µg/mL [21]. Our results confirm these statements. Absorbance spectra of CBR in interaction with CS and the corresponding calibration curve obtained from them at 570 nm are shown in Fig. 3a,b. Also, we found that the overall turbidity of CBR-CS mixtures increased linearly in the same range, as shown by the increase in the absorbance at 700 nm in Fig. 3c, related to the formation of aggregates and consequent increase in the light scattering as shown above.

A closer view to the CBR absorbance spectra shows that its wide characteristic band can be assigned to the coexistence of three different bands. This is shown in Fig. 4, where the spectrum of the dye has been decomposed in three Gaussians. The three peaks are centered at 2.228, 2.368 and 2.554 eV, respectively. Note that the mean value of both the first and the third band is almost coincident with the center of the second band. Thus, the three bands could be rationally assigned to the J-band, the monomer band, and the H-band, respectively. The relative area under the curve between the monomer band and the dimer bands (M/D) reflects the probability of the dye to undergo self-contacts in solution. At the condition of the experiment, the ratio reaches a value of 1.19, indicating an excess of monomeric dye species. The relative area under the curve of both dimer bands (H/J) reflects the geometry of the self-interaction. Since it takes a value of 1.05, a twisted

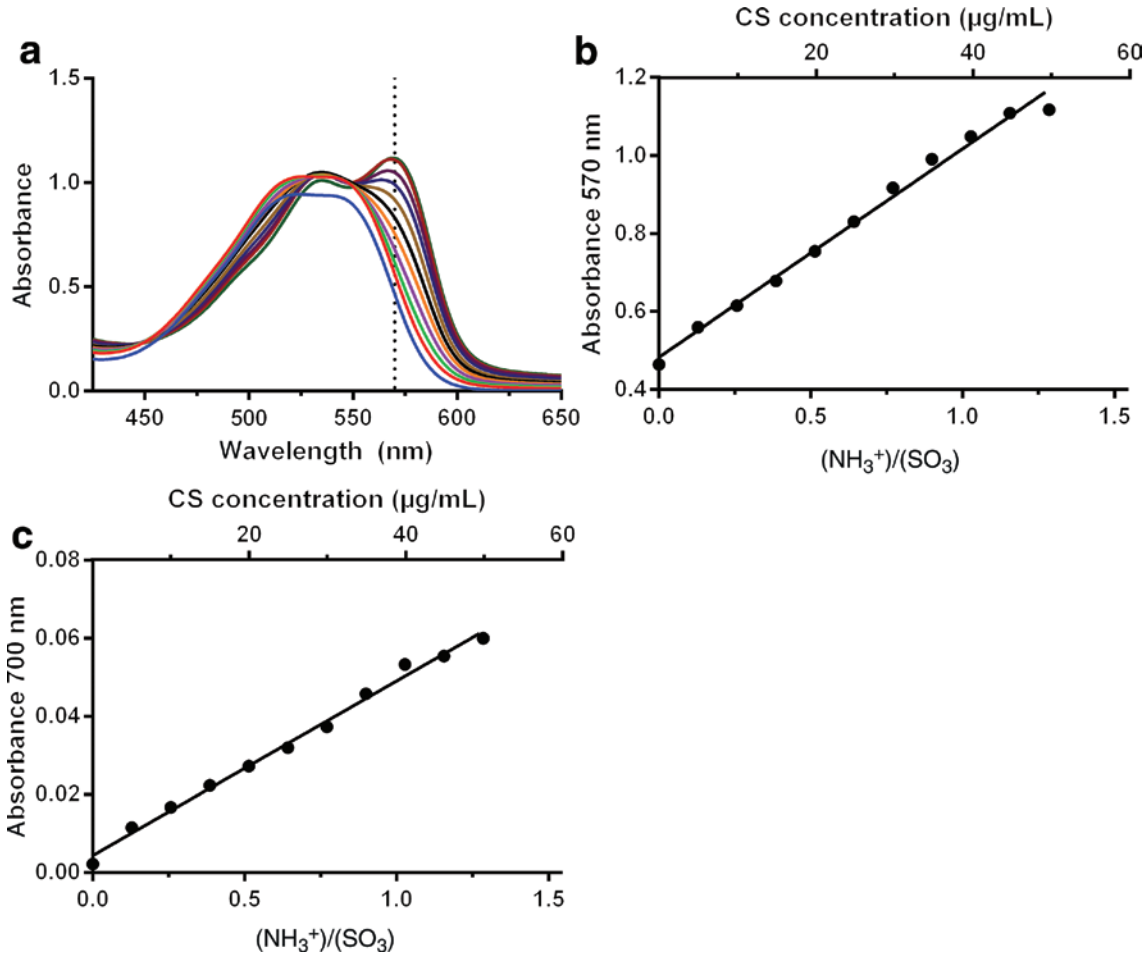

Fig. 3: (a) Absorbance spectra of CBR (0.075 g/L) in interaction with CS. (b) Absorbance at 570 nm and (c) absorbance at 700 nm versus NH_3^+/SO_3^- charge ratio and CS concentration in µg/mL, obtained from spectra shown in a.

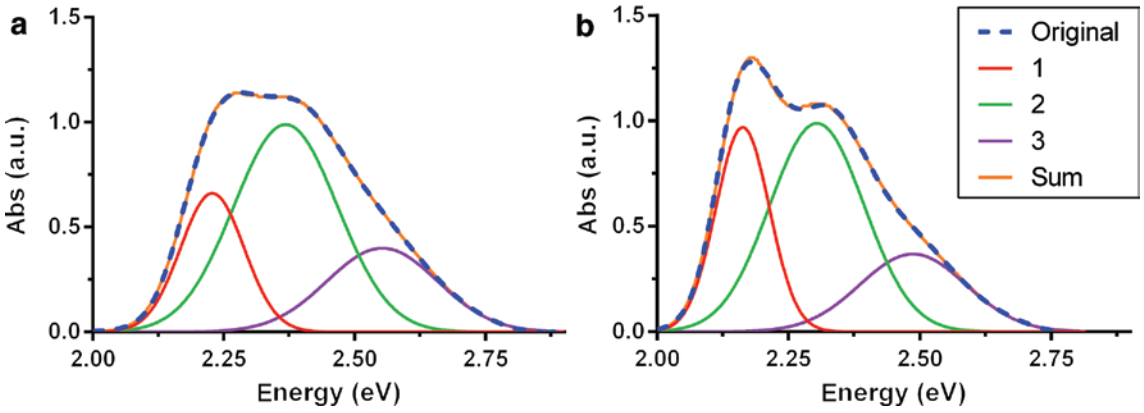

Fig. 4: Experimental absorbance spectrum, decomposed bands and their sum of (a) CBR (0.075 g/L) and (b) CBR in interaction with 50 μg/mL CS.

aggregate structure can be assumed, in which both J- and H- bands can be observed [18], that is consistent with the complex molecular structure of the dye, (see Fig. 1), which may inhibit sandwich-like stacking. In the presence of CS, the three bands are shifted to lower energies, and in the presence of 50 μg/mL of CS, they are centered at 2.164, 2.305 and 2.487 eV, respectively. The M/D value is 1.03, indicating a higher tendency to self-aggregation in the presence of the polyelectrolyte and the H/J value is 0.75, witnessing a higher contribution of the J-band. Electrostatic interaction between the negatively charged CBR and positively charged CS produces a higher concentration of the dye around the polymer, which enhances the self-stacking of CBR dye in the form of aggregates with a higher oblique character when compared to the dye in the absence of CS [13, 26]. The bathochromic shift of the whole spectrum may be due to solvatochromic effects, so that the aggregates may release part of their hydration sphere upon interaction with CS, forming ion pairs or being linked to the polymer through bound water. This is consistent with the formation of nano- and micro-complexes of both species, as shown above. However, it can be noticed in the deconvolution spectra that the J-band appears as a narrower band, which may indicate a more definite configuration of the aggregate.

Aggregation of dyes has previously shown to alter their fluorescence behavior. H-aggregation has been linked to fluorescence quenching while J-aggregates can emit, although exceptions from these rules are also reported [27]. CBR fluorescence was briefly described in a patent on the "In-Line Derivatization Of Polyaminosaccharide Polymer For Analytical Determination" [28]. The patent claims that without CS, CBR did not show any fluorescence emission while in the presence of the polymer a fluorescence peak at an emission wavelength of 600 nm and an excitation wavelength of 575 nm developed [28]. We performed further analysis of CBR and CBR in interaction with increasing CS concentrations by identifying peaks in 3D fluorescence scans (data not shown) and recording emission scans of the peaks we identified which are shown in Fig. 5.

Firstly, a very narrow peak that linearly increased with increasing CS concentration was always located at twice the excitation wavelength. This peak can be explained by second order transmission through the emission monochromator in turbid samples [29]. Figure 5c shows that the trend of the intensity of this peak with increasing CS concentrations very closely resembles size measurements and count rate trends shown in the DLS experiments which gives further evidence on the colloidal stability of the aggregates which is minimized at NH_3^+/SO_3^- charge ratios where aggregates have shown a high size and neutral zeta potential.

A non-linear gain in fluorescence intensity was found at an excitation wavelength of 570 nm, and its intensity versus CS concentration is shown in Fig. 5c. The excitation wavelength is related to the peak whose intensity also increases at high concentrations of CS, and confirms the results described in the previously mentioned patent [28]. J-aggregates of dyes have been shown to have fluorescence emission that can exceed that of monomeric dyes [27]. Dye aggregation, in general, is often linked to quenching of fluorescence which has been named aggregation-caused quenching (ACQ). Since in this case the fluorescence emission was increased with CS concentration, and therefore aggregation, we can consider this a case of aggregation-induced emission (AIE). In AIE a weakly or non-fluorescent dye emits stronger in its aggregated

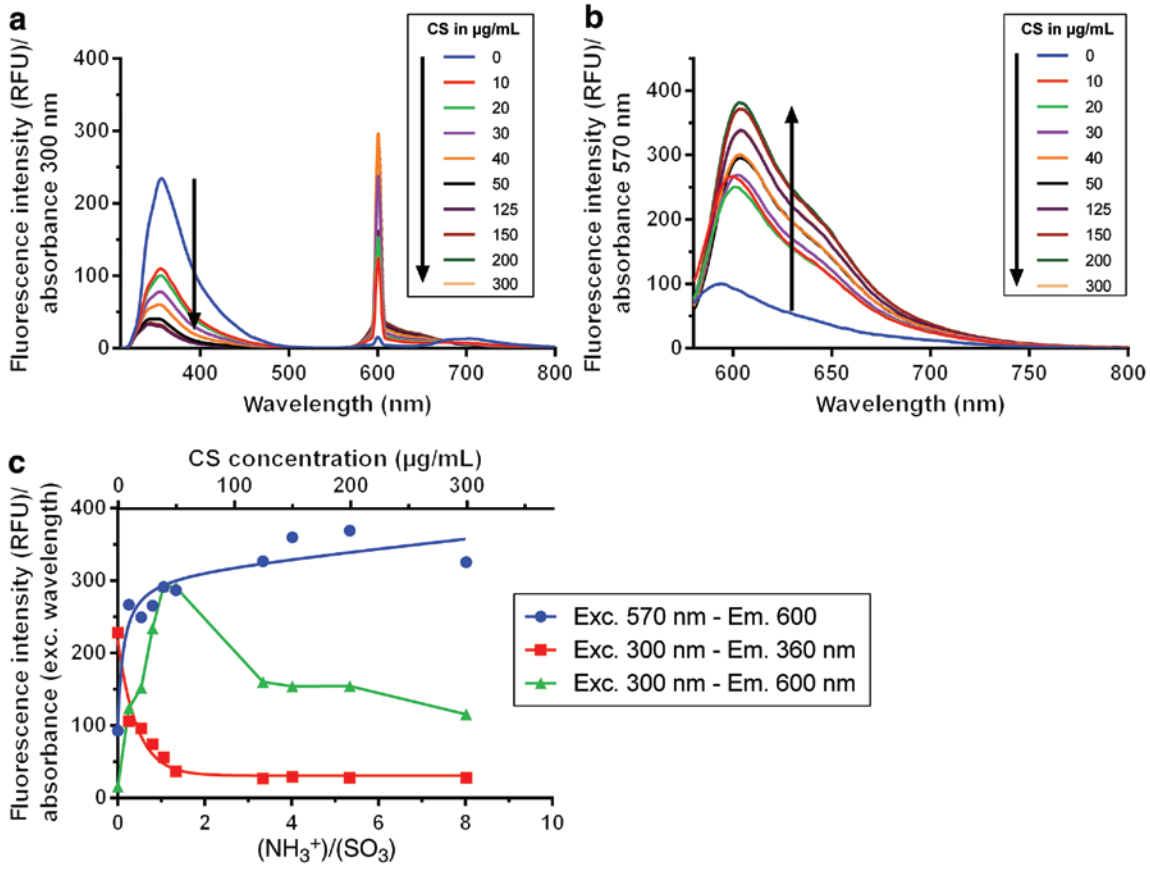

Fig. 5: Fluorescence emission spectra with an excitation wavelength of (a) 300 nm (b) 570 nm of CS (amount shown in legend in µg/mL) in interaction with CBR (fixed at 0.075 g/L). (c) Fluorescence intensity of peaks in a and b versus NH_3^+/SO_3^- charge ratio (bottom x-axis) and CS concentration (top x-axis), $\lambda_{ex} = 300$ nm, $\lambda_{em} = 360$ nm with one-phase decay fit ($R^2 = 0.96$), $\lambda_{ex} = 570$ nm, $\lambda_{em} = 600$ nm with binding saturation fit ($R^2 = 0.91$).

form. Figure 5b and c show that the AIE showed a strong non-linear increase at low CS concentrations compared to the dye alone, while the emission only increased slightly at higher CS concentrations. Research on AIE has received wide attention in the recent years, and it has been proposed that AIE has a large potential in biomedical applications [30–33]. In a particularly relevant study CS has been chemically modified with an AIE label and tracked upon aggregation inside cells for as long as 15 passages while not contaminating other cell lines in co-culture [34]. CBR could be a promising fluorescence label for future studies of CS, which fluoresces when aggregated with CS.

Lastly, a strong emission at $\lambda_{em} = 360$ nm was observed with the dye in dilute solutions of the dye at excitation wavelengths in the range of $\lambda_{ex} = 240–325$ nm. This emission was quenched upon interaction with CS and therefore showing ACQ, in contrast to the AIE described before. Further investigation of this quenching behavior (Fig. 5a and c) showed that quenching was not linear with CS concentration and reached its base level at a ratio of ~1.0.

The origin of ACQ and AIE peaks could stem on the same fluorophore. The absorbance peak at around 270 nm is attributed to a $S_0 \rightarrow S_2$ transition, while that at around 525 nm to a $S_0 \rightarrow S_1$ transition. Interaction with CS and release of part of the hydration sphere changes the relative energies of S_0, S_1 and S_2, their relative frequency of intersystem crossing, and thus, the relative frequency of radiative and non-radiative relaxation mechanisms. On the other hand, it could also be considered that both absorption bands may be due to different chromophores experiencing different photophysical effects upon aggregation.

Due to the chiral nature of CS, circular dichroism (CD) analyses were performed to study the chirality of CBR aggregates on the PEL. The results are presented in Fig. 6. The circular dichroism spectra have shown that

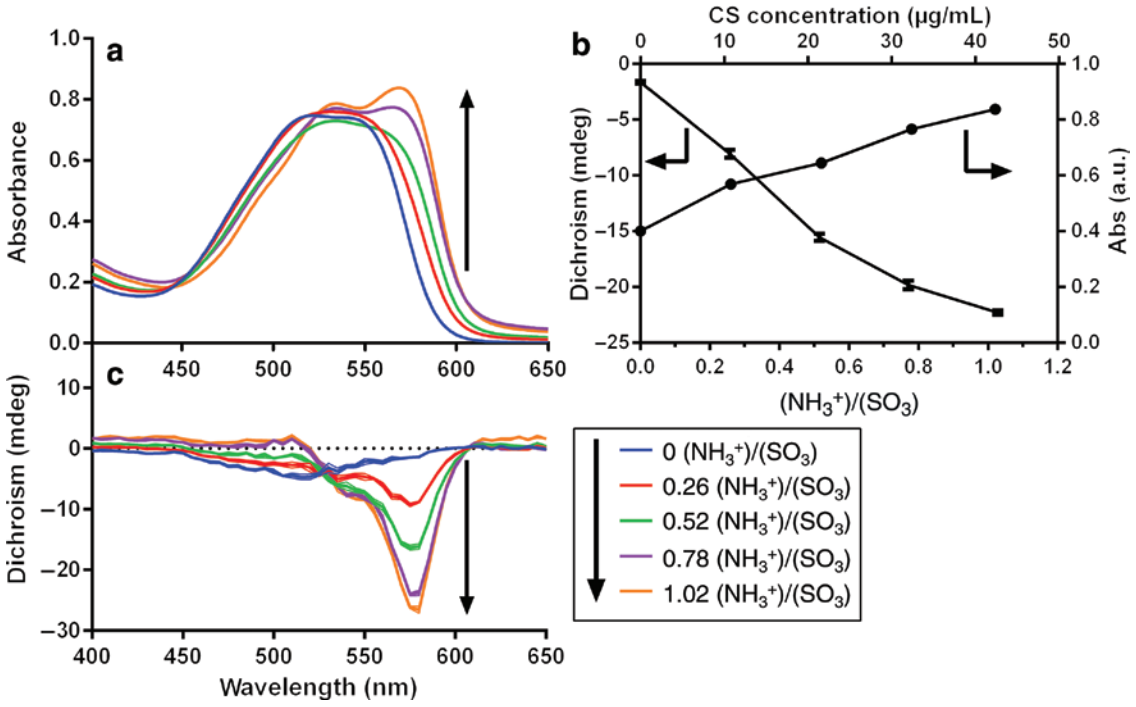

Fig. 6: (a) Absorbance spectra, (c) circular dichroism spectra of CBR (0.075 g/L) in glycine HCl buffer (pH 3.22, 0.1 M) during interaction with different amounts of added CS expressed in NH_3^+/SO_3^- charge ratio. (b) Dichroism and absorbance at 570 nm versus NH_3^+/SO_3^- charge ratio.

CBR in glycine-HCL buffer only exhibited a minor negative dichroism signal compared to the buffer alone. By increasing the CS concentration in the solution a concentration dependent negative Cotton effect was observed, with an inversion point at 530 nm. The absorbance and dichroism signal at 570 nm both showed a linear correlation with NH_3^+/SO_3^- molar charge ratio up to a ratio of 1.0, after which the absorbance increase/dichroism signal decrease seemed to taper off. It is interesting to notice that the strongest signal corresponds to the J-band, related to the head-to-tail geometry of the aggregate that may coil around the CS chain.

Pal and Pal observed a similar negative Cotton-effect and proposed a staggered aggregation and systematic twists or a helical array of chitosan hydrochloride in interaction with eosin [35]. The molecular structure of CS in solution remains experimentally unverified, although computational studies have been performed. Chitosan exhibited a highly pH and DA-dependent structure, demonstrating a relaxed two-fold (right-handed) or five-fold (left-handed) helical structure at low pH and low DA. At higher pH or high DA, the structure more closely resembles the two-fold structure of crystalline chitin [36, 37]. A uniform distribution of acetyl groups in intermediate DA CSs also exhibited a higher probability of a relaxed two-fold or five-fold helix while CSs with blockwise distributions of acetyl groups exhibited a two-fold structure [37]. The negative Cotton effect induced by CS in interaction with eosin [35] or with CBR in this study suggest a left-handed helical motif according to the Exciton Chirality Method [38, 39]. However, it is possible that the interaction with the dye either stabilizes one of the two suggested native conformations or even introduces a different left-handed helical structure that CS does not exhibit on its own in solution at low pH. Further studies could investigate in greater detail the effect of DA and pattern of acetylation on the circular dichroism signal of CBR to obtain experimental evidence for the computationally demonstrated effect of DA and pattern of acetylation.

Influence of polymer structure on changes induced in CBR

With a view to elucidating the influence of the molecular structure of the PEL interacting with CBR on its photophysical behavior, two experiments with substrates other than CS were performed. Figure 7 shows

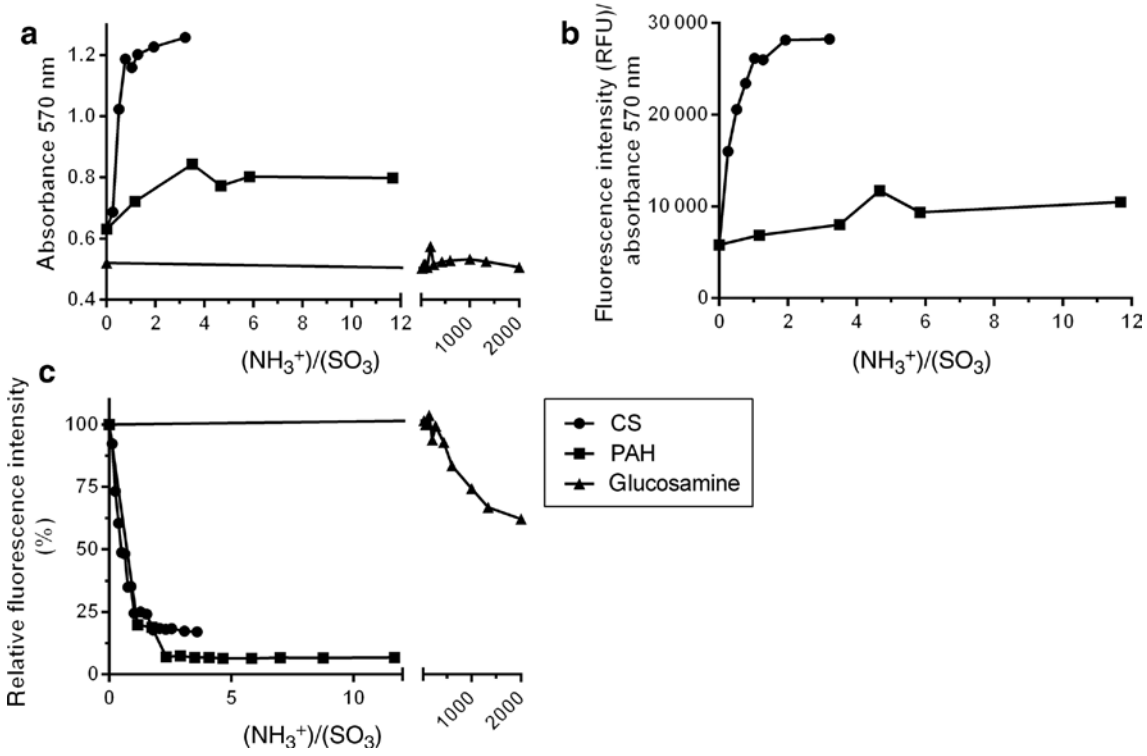

Fig. 7: (a) Absorbance at 570 nm, (b) corrected fluorescence intensity (λ_{ex} = 570 nm, λ_{em} = 600 nm), (c) relative fluorescence intensity (λ_{ex} = 300 nm, λ_{em} = 360 nm) versus ratio of NH_3^+ residues of CS, PAH and glucosamine (see Legend) to SO_3^- residues of CBR. Measurements performed using glycine HCl-buffer (pH 3.22, 0.1 M) and a fixed CBR concentration of 0.075 g/L.

a comparison of the influence of the positively charged monomer of chitosan, glucosamine and another polymer containing a positively charged amino group, poly(allylamine) hydrochloride (PAH) with CS on the absorbance and fluorescence behavior of CBR. Glucosamine showed no significant influence on the absorbance at 570 nm of CBR, even at extremely high charge ratios compared to CS. With CS, CBR absorbance increased rapidly between ratios of 0 and 1, after which it stayed relatively constant at ≈1.2. Fluorescence at λ_{ex} = 300 nm and λ_{em} = 360 nm showed slight non-linear decay in the presence of glucosamine at concentrations much higher than in the presence of CS.

Previous studies have found PEL – dye interactions to be strongly influenced by the molecular weight of the PEL [40–42]. Our experiments have shown that the same is true for CBR and CS, where the monomer that should be able to electrostatically interact with the dye only barely changes its photophysical behavior. Pal and Chaudhuri and others state that while electrostatic interactions are important in PEL – dye interactions, ultimately, the spectral changes are due to dye-dye interactions of dye molecules bound electrostatically to the PEL [41, 43]. The hypothesis that the conformation of the polymer has an influence on the interaction is supported by the changes in circular dichroism signal previously discussed.

To further elucidate the influence of polymer structure on the photophysical response of CBR in Fig. 7 we also investigated the influence of another polymer containing a positively charged amino group, namely poly(allylamine) hydrochloride (PAH). Other than the mere presence of amino groups, CS and PAH are structurally very different, with PAH not possessing saccharide units and a higher linear charge density and an intrinsically much greater chain flexibility. Figure 8a shows that the whole CBR spectrum is shifted to lower energies in the presence of PAH, as in the case of in the presence of CS, showing a very similar pattern. Figure 9 shows, in addition, that CBR and PAH formed micro- to nanoparticles depending on their NH_3^+/SO_3^- charge ratio, with size, zeta potential and derived count rate following the trends showed previously for CS and CBR. However, Figs. 7 and 8a demonstrate that the structural differences between both polyelectrolytes make a difference in the CBR absorbance intensity at 570 nm, which reached saturation at lower absorbance

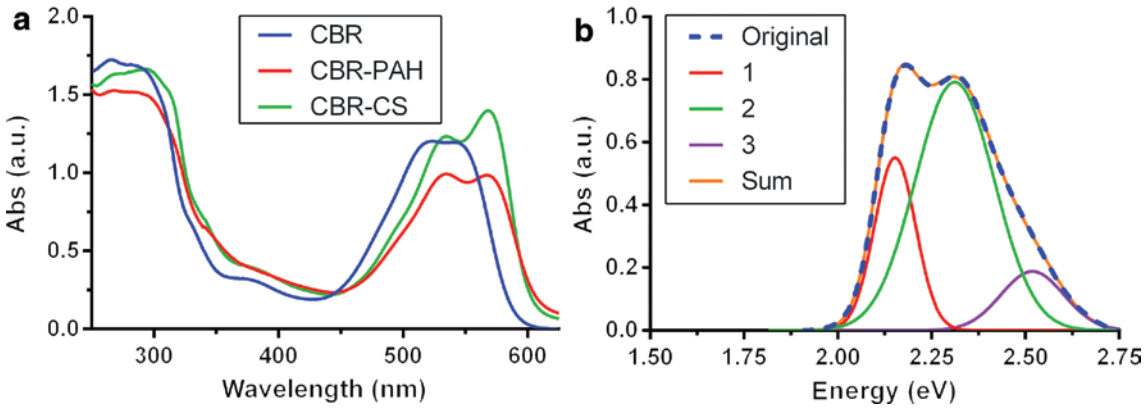

Fig. 8: (a) Absorbance spectra of CBR and CBR in interaction with 50 µL/mL CS or PAH. (b) Experimental absorbance spectrum (original), decomposed bands (1, 2 and 3) and their sum of CBR in interaction with 50 µg/mL PAH.

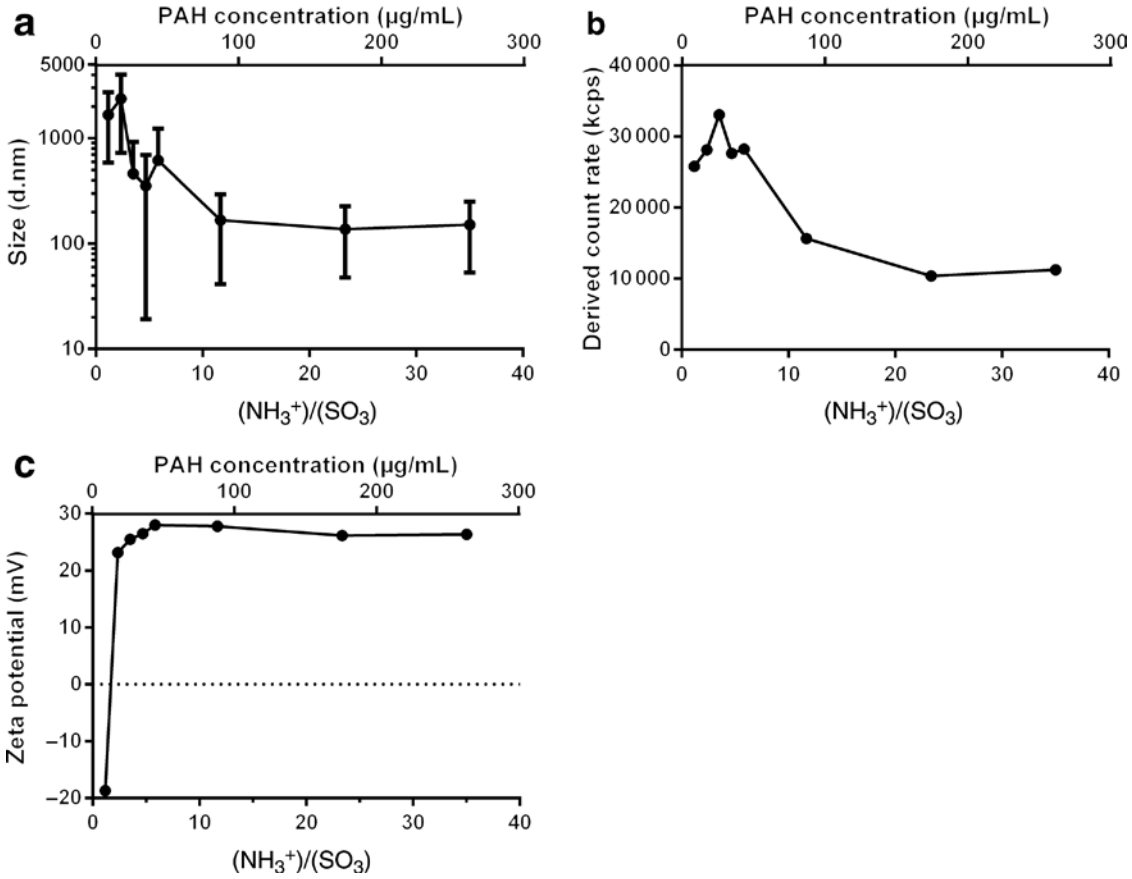

Fig. 9: (a) Size of CBR – PAH complexes with standard deviation showing polydispersity in nanometers (PDI width), (b) derived count rate, (c) zeta potential versus NH_3^+/SO_3^- ratio. All measurements performed with 0.075 g/L CBR in glycine-HCl buffer (pH 3.22, 0.1 M) with varying concentrations of PAH, expressed in NH_3^+/SO_3^- charge ratio and concentration.

values when it interacted with PAH as compared to CS. As can be seen in Fig. 7b, the corresponding spectra after deconvolution showed a J-band wider than in the presence of CS. Also, the separation between the H and the J- bands are smaller than in the presence of the polysaccharide, so that higher overlapping with the monomer band produces a less notorious increase of the signal at 570 nm (2.175 eV). In the presence of 50 µg/mL of PAH, the J-, monomer, and H-bands are centered at 2.153, 2.311 and 2.520 eV, respectively. The

M/D value is 1.81, indicating a much lower tendency to self-aggregation in the presence of this polyelectrolyte than in the presence of CS or in the absence of any of both polyelectrolytes. The H/J value is 0.52, lower than in the presence of CS or for pristine CBR, indicating a higher oblique character of the aggregates, caused both by a decrease of the θ angle or an increase of the α angle. While the relative contribution of the J-band is higher when CBR interacts with PAH than with CS, the total contribution of dimeric dye species is much lower. The analytical efficacy of CBR for PEL solutions, therefore, depends on a balance of aggregation and contribution of the J-band in the aggregates, which makes the band at 570 nm distinguishable. In connection with this, the aggregation induced emission, previously demonstrated with CS, is much weaker when CBR was in interaction with PAH, related with a lower contribution of dimeric species to the total absorbance spectrum. On the other hand, fluorescence quenching of the band at 360 nm was found equally strong in PAH and CS.

Final remarks

Several photophysical changes that can be induced in CBR using CS or other substrates that were previously unreported have been presented which allow us describing specific features of the interaction. The interaction of CBR with the cationic PELs CS and PAH produced a bathochromic shift of the dye spectrum, due to enhanced aggregation upon electrostatic interaction, and release of water from its hydration sphere, thus providing a different microenvironment. Due to this aggregation, nano- and microcomplexes are formed, depending on the relative charge ratio. Strongly fluctuating sizes and zeta potentials of the aggregates depending on the NH_3^+/SO_3^- ratios and correlating count rate measurements in DLS and scattering peaks in fluorescence show that aggregates experience colloidal stabilization in different extent. We therefore recommend favoring the colorimetric method over the centrifugation method to determine concentrations of CS that could be outside the linear range for the centrifugation method (20 μg/mL) since the aggregates are potentially stabilized by their low size and high zeta potential at high contents of the PEL, thus inducing to errors in the measurement of free dye after centrifugation.

Fluorescence quenching in the low wavelength range of the spectrum, probably corresponding to a $S_0 \rightarrow S_2$ transition, is observed upon aggregation with both PELs. This quenching is also observed in the presence of high amounts of the non-polymeric D-glucosamine. Indeed, the weaker interaction with glucosamine can be explained by binding cooperativity in electrostatic interactions [44] and cooperativity of stacking interaction that requires a minimal critical chain length, as shown in other PEL – dye interactions [40, 42].

In contrast to the fluorescence quenching, a fluorescence AIE around 570 nm has been found to be stronger for CS than for PAH. The fluorescence can be related to the J-band corresponding to oblique head-to-tail aggregates, which are favored in the presence of CS over than in the presence of PAH. Indeed, the difference in the increase of the absorbance intensity at 570 nm and AIE in PAH and CS can be explained by the different extent of molecular aggregation, higher regularity of the aggregate structure that makes the band narrower, and the different orientation determined by the θ and α angles. The chiral conformation and low linear charge density of the polysaccharide CS where the amino groups are oriented at opposite sides of the chain axis facilitates an elongated configuration of stacked dyes, which makes CBR ideal for the determination of CS concentrations.

We suggest that the spectral changes in CBR could have a practical significance for concentration determination of other amino group containing polymers or possibly even positively charged polymers in general. The wavelength shift would have to be determined for every polymer individually, and sensitivity will depend on the polymer structure. About CS, we propose that further study could explore the effect of degree and pattern of acetylation of CS on the interaction with CBR since these parameters determine the charge density that CBR seems to be sensitive to, which could expand the use of the CBR – CS interaction in the future.

Conclusion

In summary new insights into the CBR-PELs interaction, and more specifically into the CBR – CS interaction, have been established by studying their interaction using previously unused techniques, namely DLS-NIBS, M3-PALS and CD. CBR formed nano- to microaggregates with PELs such as CS and PAH, depending on their charge ratio. At low and high PEL – CBR ratios these aggregates are stabilized by their zeta potential, whereas at ratios around 1.0 they show neutral zeta potential, large sizes and become unstable. The aggregation of CBR to the PELs induces several photophysical changes in CBR that were observed by different spectroscopic methods. H- and J-bands appear in the spectra of the pristine dye, and in interaction with CS and PAH. A bathochromic absorbance shift of the whole spectra has been shown in the presence of the PELs, showing a clear signal at 570 nm, which witnesses a different microenvironment for the dye, and is consistent with the formation of the nano and micro-complexes. CBR in solution shows strong fluorescence when excited in the range of $\lambda_{ex} = 250–300$ nm, $\lambda_{em} = 360$ nm that is quenched upon interaction with CS or PAH. Interestingly, CBR showed aggregation induced emission at $\lambda_{ex} = 570$ nm, $\lambda_{em} = 600$ nm. The relative intensity of the H- and the J-bands in the presence of both PELs indicate that an enhanced oblique head-to-tail stacking of CBR molecules is produced in the presence of CS or PAH when comparing to the pristine dye. However, a greater extent of aggregation has been found in the presence of CS when comparing to the case in the presence of PAH, and the separation and definition of the J-band from the monomer band is higher in the case of CS. Thus the absorbance intensity at 570 nm, associated to the J-band, and the related, more intense induced emission can rationally be used for CS concentration determination. The induced emission could also be exploited as CS label. Additionally, induced circular dichroism showed enhanced negative Cotton signs at 570 nm as a specific feature of the CS – CBR interaction. On this basis, we proposed a left-handed helical arrangement of dye on CS that was previously anticipated by *in silico* studies on CS in solution.

Acknowledgments: We acknowledge support from DFG, Germany (Project GRK 1549 International Research Training Group 'Molecular and Cellular GlycoSciences'), the research leading to these results has also received funding from the European Union's Seventh Framework Programme for research, technological development and demonstration under grant agreement no. 613931 (Nano3Bio). We also thank Fondecyt Regular (Grants No. 1120514 and 1150899, Conicyt, Chile) for financial support. We are indebted to Prof. Michael Hippler for the use of the fluorometer and Prof. Peter Bruckner and Prof. Johannes Eble (Uniklinikum Münster) for generous access to CD instrument.

References

[1] S. Dai. in *Cationic Polym. Regen. Med.* S. Samal, P. Debruel (Eds.), pp. 557–582, The Royal Society of Chemistry, Cambridge, United Kingdom (2015).
[2] A. F. Kotzé, H. L. Lueßen, B. J. de Leeuw, (A)Bert G de Boer, J. Coos Verhoef, H. E. Junginger. *J. Control. Release* **51**, 35 (1998).
[3] M. Rinaudo. *Prog. Polym. Sci.* **31**, 603 (2006).
[4] E. Fröhlich. *Int. J. Nanomedicine* **7**, 5577 (2012).
[5] B. D. Gummow, G. A. F. Roberts. *Die Makromol. Chemie* **186**, 1239 (1985).
[6] M. Schubert, D. Hamerman. *J. Histochem. Cytochem.* **4**, 159 (1956).
[7] I. Moreno-Villoslada, J. P. Fuenzalida, G. Tripailaf, R. Araya-Hermosilla, G. D. C. Pizarro, O. G. Marambio, H. Nishide. *J. Phys. Chem. B* **114**, 11983 (2010).
[8] I. Moreno-Villoslada, C. Torres-Gallegos, R. Araya-Hermosilla, H. Nishide. *J. Phys. Chem. B* **114**, 4151 (2010).
[9] I. Moreno-Villoslada, C. Torres, F. González, T. Shibue, H. Nishide. *Macromol. Chem. Phys.* **210**, 1167 (2009).
[10] M. Gómez-Tardajos, J. P. Pino-Pinto, C. Díaz-Soto, M. E. Flores, A. Gallardo, C. Elvira, H. Reinecke, H. Nishide, I. Moreno-Villoslada. *Dye. Pigment.* **99**, 759 (2013).
[11] Roger W. Kugel. *Structure-Property Relations in Polymers*, American Chemical Society, Washington, DC (1993).
[12] E. E. Jelley. *Nature* **138**, 1009 (1936).
[13] M. Kasha. *Radiat. Res.* **20**, 55 (1963).
[14] T. Katoh, Y. Inagaki, R. Okazaki. *Bull. Chem. Soc. Jpn.* **70**, 2279 (1997).

[15] A. Mishra, R. K. Behera, P. K. Behera, B. K. Mishra, G. B. Behera. *Chem. Rev.* **100**, 1973 (2000).
[16] K. Patil, R. Pawar, P. Talap. *Phys. Chem. Chem. Phys.* **2**, 4313 (2000).
[17] I. Willerich, H. Ritter, F. Gröhn. *J. Phys. Chem. B* **113**, 3339 (2009).
[18] V. Martínez Martínez, F. López Arbeloa, J. Bañuelos Prieto, T. Arbeloa López, I. López Arbeloa. *J. Phys. Chem. B* **108**, 20030 (2004).
[19] R. N. Puri, R. Roskoski. *Arch. Biochem. Biophys.* **303**, 288 (1993).
[20] S. Subramanian, P. D. Ross. *Crit. Rev. Biochem. Mol. Biol.* **16**, 169 (1984).
[21] R. A. A. Muzzarelli. *Anal. Biochem.* **260**, 255 (1998).
[22] B. Miralles, M. Mengíbar, R. Harris, A. Heras. *Food Chem.* **126**, 1836 (2011).
[23] A. Mendelovits, T. Prat, Y. Gonen, G. Rytwoa, G. Rytwo, G. Rytwoa, G. Rytwo. *Appl. Spectrosc.* **66**, 979 (2012).
[24] M. Wojdyr. *J. Appl. Crystallogr.* **43**, 1126 (2010).
[25] C. Wischke, H.-H. Borchert. *Carbohydr. Res.* **341**, 2978 (2006).
[26] M. Kasha, H. R. Rawls, M. Ashraf El-Bayoumi. *Pure Appl. Chem.* **11**, 371 (1965).
[27] U. Rösch, S. Yao, R. Wortmann, F. Würthner. *Angew. Chem.* **118**, 7184 (2006).
[28] J. Qian, P. Brister. US20120164742 A1 (28 June 2012).
[29] J. R. Lakowicz. *Principles of Fluorescence Spectroscopy*, Springer US, New York, USA (2006).
[30] J. Luo, Z. Xie, J. W. Y. Lam, L. Cheng, B. Z. Tang, H. Chen, C. Qiu, H. S. Kwok, X. Zhan, Y. Liu, D. Zhu. *Chem. Commun.* 1740 (2001).
[31] M. Yang, D. Xu, W. Xi, L. Wang, J. Zheng, J. Huang, J. Zhang, H. Zhou, J. Wu, Y. Tian. *J. Org. Chem.* **78**, 10344 (2013).
[32] M. C. Gather, S. H. Yun. *Nat. Commun.* **5**, 5722 (2014).
[33] J. Mei, Y. Hong, J. W. Y. Lam, A. Qin, Y. Tang, B. Z. Tang. *Adv. Mater.* **26**, 5429 (2014).
[34] Z. Wang, S. Chen, J. W. Y. Lam, W. Qin, R. T. K. Kwok, N. Xie, Q. Hu, B. Z. Tang. *J. Am. Chem. Soc.* **135**, 8238 (2013).
[35] M. K. Pal, P. K. Pal. *Die Makromol. Chemie, Rapid Commun.* **9**, 237 (1988).
[36] E. F. Franca, R. D. Lins, L. C. G. Freitas, T. P. Straatsma. *J. Chem. Theory Comput.* **4**, 2141 (2008).
[37] E. F. Franca, L. C. G. Freitas, R. D. Lins. *Biopolymers* **95**, 448 (2011).
[38] N. Harada, K. Nakanishi. *Acc. Chem. Res.* **5**, 257 (1972).
[39] R. A. Garoff, E. A. Litzinger, R. E. Connor, I. Fishman, B. A. Armitage. *Langmuir* **18**, 6330 (2002).
[40] K. Yamaoka, M. Takatsuki, K. Yaguchi, M. Miura. *Bull. Chem. Soc. Jpn.* **47**, 611 (1974).
[41] Q. C. Jiao, Q. Liu, C. Sun, H. He. *Talanta* **48**, 1095 (1999).
[42] M. Shirai, T. Nagatsuka, M. Tanaka. *J. Polym. Sci. Polym. Chem. Ed.* **15**, 2083 (1977).
[43] M. K. Pal, M. Chaudhuri. *Die Makromol. Chemie* **133**, 151 (1970).
[44] D. Horn, C. C. Heuck. *J. Biol. Chem.* **258**, 1665 (1983).